Dynamical Discrete/Continuum Linear Response Shells Theory of Solvation: Convergence Test for NH_4^+ and OH^- Ions in Water Solution Using DFT and DFTB Methods

Guilherme Ferreira de Lima,[†] Hélio Anderson Duarte,[†] and Josefredo R. Pliego, Jr.*[,‡]

Grupo de Pesquisa em Química Inorgânica Teórica (GPQIT), Departamento de Química, ICEx, Universidade Federal de Minas Gerais, 31270-901, Belo Horizonte, MG, Brazil, and Departamento de Ciências Naturais, Universidade Federal de São João del-Rei, 36301-160, São João del-Rei, MG, Brazil

Received: October 25, 2010

A new dynamical discrete/continuum solvation model was tested for NH_4^+ and OH^- ions in water solvent. The method is similar to continuum solvation models in a sense that the linear response approximation is used. However, different from pure continuum models, explicit solvent molecules are included in the inner shell, which allows adequate treatment of specific solute−solvent interactions present in the first solvation shell, the main drawback of continuum models. Molecular dynamics calculations coupled with SCC-DFTB method are used to generate the configurations of the solute in a box with 64 water molecules, while the interaction energies are calculated at the DFT level. We have tested the convergence of the method using a variable number of explicit water molecules and it was found that even a small number of waters (as low as 14) are able to produce converged values. Our results also point out that the Born model, often used for long-range correction, is not reliable and our method should be applied for more accurate calculations.

Introduction

Theoretical calculations have become an important tool in the investigation of chemical phenomena, providing new insights and contributing to interpretation of experimental results. Reliable molecular calculations are now affordable using methods such as density functional theory (DFT), Moller−Plesset perturbation theory (MP2, MP4), and coupled-cluster (CCSD(T)). For large systems, approximate methods, such as semiempirical and, more recently, the density functional-tight binding (DFTB)[1] methods are available. While it is possible to describe very accurately chemical processes in the gas phase, many important chemical reactions occur in the liquid phase and the solvent has an important role both in the thermodynamics and in the kinetics of reactions.[2–12] In this way, many recent theoretical researches have focused in the development of methods for describing solvation.[2–26]

Continuum solvation models[12,25,27] such as the popular polarized continuum model[11,28] and the SMx family[22,24,29–32] are the first-line approaches used for including solvent effects. In continuum models the solute molecule is placed in a cavity inside a dielectric with the dielectric constant of the solvent. The interaction between the dielectric and the solute molecule gives the solvation free energy. The different ways of creating the cavity, its shape, the solute charge distribution, and the nonelectrostatic terms lead to the different continuum models. Recent studies have pointed out that, for neutral molecules, the theoretical solvation free energies have an average error lower than 1 kcal mol^{-1} when compared to experimental data.[24,33] However, for ionic species, to achieve an error lower than 4 kcal mol^{-1} remains a very difficult task. In fact, small differences in the cavity definition can lead to large variation in the solvation energy of ions.[5] It has been argued that describing the first solvation shell is the main weakness in continuum models due to specific solute−solvent interactions.[4] Although the dielectric continuum provides a good description of the bulk solvent, it is not able to describe the interaction between the solute and the first solvation shell.

Continuum solvation models can be improved through their combination with explicit solvent molecules.[4,34] These models are called hybrid models. The main problems of hybrid models are how to calculate the solvation free energy and how many solvent molecules should be introduced. One approach is the cluster-continuum[4] model of Pliego and Riveros, which is very similar to quasi-chemical theory[35–37] of solvation of Pratt and co-workers. In this approach, some solvent molecules are strategically positioned to describe the specific interaction between the solute and the solvent and the long-range effects are described through the dielectric continuum. In order to calculate the solvation free energy, the cluster is considered a chemical species. These hybrid methodologies were used to study the solvation of species like OH^-,[36] Be^{2+},[35] K^+,[38] and others[4,6,33,37,39] in different solvents. Hybrid models combined with gas-phase calculations have been used to calculate pK_a[33,34,40–45] and redox[42,43,45] potential, obtaining good agreement with the experimental data for both organic and inorganic species. Although hybrid methods produce good results, many questions about the influence of the explicit solvent molecules are still open and were recently pointed out by Zhao et al.[46] How many solvent molecules must be used to describe the specific interaction? Is the optimized cluster a good approach to describe the species in solution at room temperatures? Can just one structure describe all system in solution? Dynamical hybrid discrete-continuum solvation models have been proposed to address these questions.[9,10,21]

The most realistic approach for describing solvation would be using explicit solvent molecules combined with molecular dynamics simulation or Monte Carlo method. Thus, these methods can be coupled with free energy perturbation, thermodynamic integration, or even linear response approximation[47–50] for calculating the solvation free energy. However, classical

* Corresponding author. E-mail: pliego@ufsj.edu.br.
[†] Universidade Federal de Minas Gerais.
[‡] Universidade Federal de São João Del Rei Campus Dom Bosco.

10.1021/jp110202e
Published on Web 11/15/2010

force fields are not always reliable and full quantum-mechanical calculations are computationally very demanding.

In the present paper, we have explored a new dynamical hybrid discrete/continuum solvation method proposed by Pliego in a recent work.[51] Our aim is to analyze a linear response version and to test the convergence of the method in relation to the number of solvent molecules using SCC-DFTB and DFT calculations for explicit solvent molecules, and PCM for the long-range interactions. A brief description of the theory will be presented in the next section and in the following sections the method is applied for the NH_4^+ and the OH^- ions in water solvent.

Theory

The idea underlying the shells theory of solvation is that the interaction between the solute (A) and the solvent molecules (S) can be decomposed, considering the interaction with two (or even more) shells. The inner shell (S_1) is in the closest contact with the solvent while the outer shell (S_2) describes the remaining bulk solvent. Considering the general expression of the solvation free energy for a solute A interacting with the solvent S, presented below

$$\Delta G_{solv}(A) = -RT \ln \frac{\int e^{-\beta(U_{AS_1}+U_{AS_2}+U_{AS_1S_2})} e^{-\beta(U_{S_1}+U_{S_2}+U_{S_1S_2})} \mathbf{dr_1}\, \mathbf{dr_2}}{\int e^{-\beta(U_{S_1}+U_{S_2}+U_{S_1S_2})} \mathbf{dr_1}\, \mathbf{dr_2}} \quad (1)$$

and using a set of approximations,[51] it is possible to arrive at the following expression:

$$\Delta G_{solv}(A) = \Delta G_{solv,R}(A) + \frac{1}{2}\left(\langle U_{AS_1}\rangle_{S_1,\lambda=1} + \langle U_{AS_1}\rangle_{S_1,\lambda=0}\right) + \frac{1}{2}\langle \Delta G_{solv}(AS_1) - \Delta G_{solv}((A)S_1)\rangle_{\lambda=1} + \frac{1}{2}\langle \Delta G_{solv}(AS_1) - \Delta G_{solv}((A)S_1)\rangle_{\lambda=0} \quad (2)$$

The first term is the cavity formation contribution, and the second term (in parentheses) corresponds to the interaction of the solute with the inner shell, with configurations generated with inclusion ($\lambda = 1$) or not ($\lambda = 0$) of the electrostatic solute−solvent interactions. The third term is the solvation of the solute + inner shell by the outer shell less the solvation of the inner shell including the solute hole, so that the solvent molecules do not reach the position of the solute A. The fourth term is similar to the third term, but now only the repulsive potential of the solute A is used in the generation of the configurations of S_1.

In the present paper, our objective was analyzing the convergence of the method in relation to number of solvent molecules, as well as to test the use of an approximation to eq 2. In this more approximate scheme, we have excluded the first term, corresponding to the cavity formation, set the $\langle U_{AS_1}\rangle_{S_1,\lambda=0}$ term to zero, and considered that the outer-shell contribution for solvation in $\lambda = 0$ and $\lambda = 1$ are close. Therefore, the final expression becomes

$$\Delta G_{solv}(A) = \frac{1}{2}\langle U_{AS_1}\rangle_{S_1,\lambda=1} + \langle \Delta G_{solv}(AS_1) - \Delta G_{solv}((A)S_1)\rangle_{\lambda=1} \quad (3)$$

Equation 3 is very simple and easy to understand. The first term corresponds to linear response approximation for the inner-shell interaction while the second term is the outer-shell contribution for solvation of the solute A. In the practical implementation, we performed a simulation considering a box with 64 water molecules and choose those n molecules in closest contact with the solute. Then, a full quantum calculation is done for the interaction of solute molecule and the closest n solvent molecules, corresponding to the $\langle U_{AS_1}\rangle_{S_1,\lambda=1}$ contribution. The $\Delta G_{solv}(AS_1)$ is the solvation of the cluster obtained through a continuum solvation model, and the $\Delta G_{solv}((A)S_1)$ contribution corresponds to calculation without the solute A, but including its cavity. Therefore, considering that continuum solvation models use the linear response approximation, the reader can notice the present method is very similar to a full continuum calculation, with an advantage that explicit solvent molecules in the closest contact with the solvent are included. Therefore, the main flaw of continuum solvation models, specific solute−solvent interactions, can be corrected. The computational details will be presented below.

Computational Details

Geometry Optimization. Density functional calculations were performed based on the linear combination of Gaussian-type orbitals-Kohn−Sham method (LCAO-KS) implemented in the Gaussian03 package.[52] The exchange-correlation (XC) expressions due to Perdew, Burke, and Ernzerhof (PBE),[53] and Becke's three-parameter exchange functional and the correlation functional of Lee, Yang, and Parr (B3LYP),[54,55] were used with the Pople's 6-31+G(d,p) basis sets. Vibrational analyses for the optimized structures with PBE and B3LYP method were performed, assuring a minimum in the PES has been found.

The approximate method self-consistent charge-density functional−tight binding (SCC-DFTB) has been used to describe the PES in Born−Oppenheimer molecular dynamics.[1,56] A "posteriori" dispersion correction (DC) to the SCC-DFTB method has been included in the calculations.[57] All SCC-DFTB geometry optimization as mentioned in the text was performed using the DFTB+ program[58] and for the DC-SCC-DFTB molecular dynamic calculations the modified version of the deMon[59] program was used.

Molecular Dynamics Calculations. Born−Oppenheimer molecular dynamic simulations were performed on a periodic cubic box of 12.5 Å consisting of a single ion and 64 water molecules. The DC-SCC-DFTB[1] method was used to describe the PES. The equilibration was performed during 500 ps of simulation. During this step, the Berendsen thermostat[60] was used to obtain the average temperature of 300 K. After the equilibration, the thermostat was removed and a production run of 500 ps of simulation with time step of 0.5 fs was done to produce the trajectories.

Solvation Free Energy Calculations. The solvation free energy of each ion was evaluated for structures with n explicit water molecules, using eq 3. The first term is the interaction between the solute and the inner solvent shell. The criteria to select the water molecules were to choose the water molecules with the smallest distance between the center of mass of the ion and the hydrogen or oxygen atom in the water molecule. We selected structures with $n = 1, 2, 3, 4, 6, 8, 14, 32, 48$, and

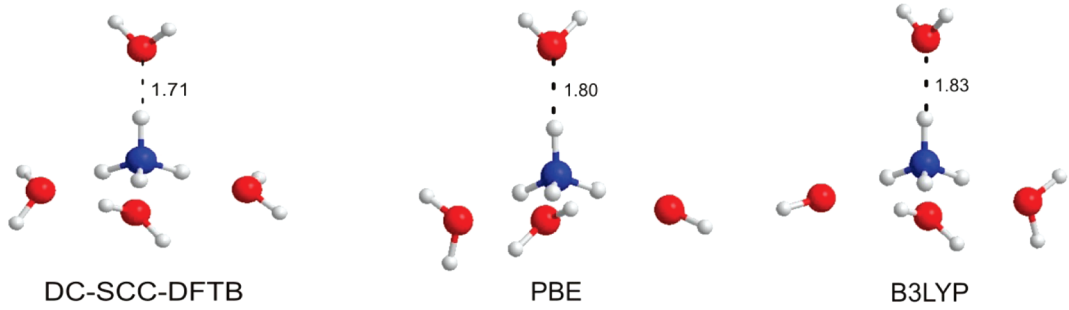

Figure 1. Structure of the $NH_4^+(H_2O)_4$ cluster obtained at DC-SCC-DFTB, PBE/6-31+G(d,p), and B3LYP/6-31+G(d,p) levels of theory.

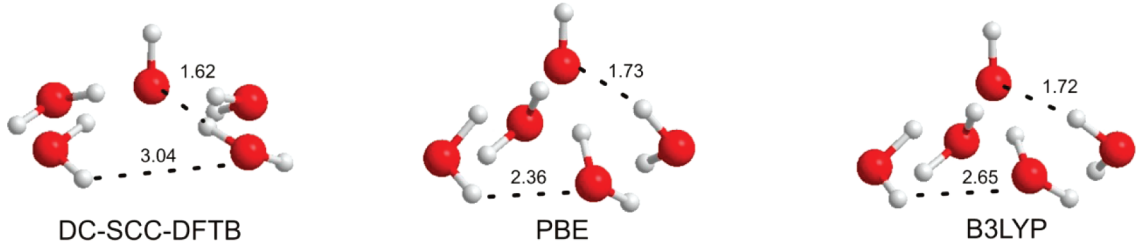

Figure 2. Structure of the $OH^-(H_2O)_4$ cluster obtained at DC-SCC-DFTB, PBE/6-31+G(d,p), and B3LYP/6-31+G(d,p) levels of theory.

TABLE 1: Interaction Energy between the Central Ion and Four Water Molecules Using Different Levels of Theory[a,b]

	interaction energy					
	NH_4^+			OH^-		
geometry	DC-SCC-DFTB	PBE	B3LYP	DC-SCC-DFTB	PBE	B3LYP
DC-SCC-DFTB	−65.82	−76.81	−74.95	−91.39	−100.60	−98.69
PBE	−64.08	−76.62	−75.16	−85.78	−94.84	−93.34
B3LYP	−62.59	−76.08	−74.70	−84.94	−94.86	−93.41

[a] Units of kcal mol^{-1}. [b] The 6-31+G(d,p) basis set was used in calculations with the PBE and B3LYP functionals.

64 water molecules. For each n value, the interaction energy was sampled upon 500 snapshots equally distributed along the trajectory, i.e., one snapshot each 1 ps, to evaluate the interaction energy using single-point PBE/6-31+G(d,p) calculations. For $n = 48$ and 64 only 200 snapshots were selected for sampling.

The long-range effects, i.e., the second term in eq 3, were evaluated using the PCM method.[11,28,61,62] Single-point PCM/RHF/6-31G(d) calculations were performed using GAMESS package[63] using the internally storage cavities and different scale factors, in the range of 1.2−2.0. For the PCM calculation we selected 20 snapshots equally spaced along the trajectory. We have chosen only 20 snapshots because the fluctuation is small and the PCM calculations for 64 water molecules are very computer intensive. As an example, if someone uses 20 snapshots, the fluctuation should not be larger than 1−2 kcal mol^{-1}.

Results and Discussion

Optimized Structures and Interaction Energies. In the first part of the work, we have analyzed the performance of DFTB method to predict geometries and interaction energies. Thus, we have investigated the $NH_4^+(H_2O)_4$ and $OH^-(H_2O)_4$ clusters using DC-SCC-DFTB, PBE/6-31+G(d,p), and B3LYP/6-31+G(d,p) methods. Figures 1 and 2 show the optimized structures obtained for each level of theory. All the methods produce similar optimized structures for the ammonium ion with four water molecules. The distance between the O (H_2O)−H (NH_4^+) obtained by the DC-SCC-DFTB method is 1.71 Å, around 0.10 Å lower than DFT geometries. However, this value is very close to 1.74 Å obtained by Zhao et al.[46] using the DFTB method in structural search via Monte Carlo simulation. In the same way, our DFTs results are also in good agreement with the reports of Intharathep et al.[64] where DFT and many ab initio methods were used.

The interaction energy between the NH_4^+ ion and the four water molecules was obtained through energy single-point calculation on the optimized cluster and considering the energy of the free ion and the water cluster with frozen geometry taken from the cluster. So, no geometry relaxation was allowed in the calculation of the fragments. The results of the interaction energy are shown in Table 1 and we can see a large dependence of the method, once the interaction energy evaluated by PBE/6-31+G(d,p) is around 10 kcal mol^{-1} more negative than that evaluated by the DC-SCC-DFTB method. On the other hand, the geometry has a small effect on the interaction energy, and the difference is not larger than 3 kcal mol^{-1}. In fact, the PBE/6-31+G(d,p)//DC-SCC-DFTB energies are very close to PBE/6-31+G(d,p)//PBE/6-31+G(d,p) values.

Optimization of the $OH^-(H_2O)_4$ cluster leads to C4 symmetry for all methods as shown in Figure 2. The distance O (OH)−H (H−O−H) evaluated at the DC-SCC-DFTB method is around 0.10 Å shorter than that obtained using DFT methods which are in good agreement with that obtained by Pliego and Riveros.[65,66] Another difference between the $OH^-(H_2O)_4$ structures optimized using the DC-SCC-DFTB method and that obtained by the DFTs methods can be observed in the H (OH)−O (OH)−H (H−O−H) angle. Pliego and Riveros[65] obtained angles around 120° using both force fields and MP2 calculations. Our results show angles of 105°, 118°, and 115° for the structures optimized using the DC-SCC-DFTB, PBE, and B3LYP, respectively. The interaction energies are listed in Table 1 and show clearly the influence of this smaller angle on

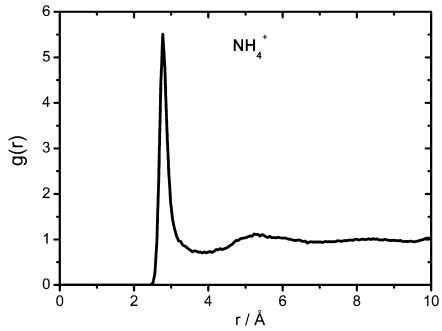

Figure 3. Radial distribution function (CM-O) for ammonium ion in water solution.

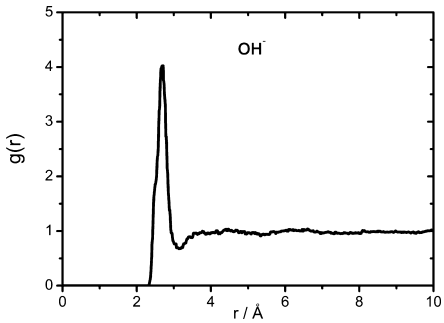

Figure 4. Distribution function (CM-O) for hydroxyl ion in water solution.

the values. The DC-SCC-DFTB optimized geometry leads to the most negative interaction energy for all the methods. Therefore, the DC-SCC-DFTB method produces good geometries for NH_4^+ cluster, but there is some performance degradation for the OH^- cluster.

Radial Distribution Function. Radial distribution functions (RDF) have been calculated for the center of mass of the solute and the oxygen of the water molecules. The ammonium ion RDF shows a minimum around 3.8 Å (Figure 3) with 8 water molecules. Intharathep et al.[64] obtained 6 water molecules using a QM/MM molecular dynamics simulation, and Brugé et al.[67] obtained 5.3 water molecules using an ab initio Car−Parrinello molecular dynamic simulation. This difference between these calculations can be attributed to a very flat minimum around 3.6−4.0 Å which produces large differences in the coordination number. Four water molecules are interacting strongly with the hydrogen of the ammonium. Other water molecules can interact directly with the ammonium; however, this interaction is weaker than the interaction with the four water molecules directed to hydrogen atom. The hydroxyl RDF (Figure 4) has a well-defined minimum in 3.1 Å with four water molecules coordinating to the hydroxyl anion. Our results are in good agreement with the results obtained by Asthagiri el al.[68] using ab initio molecular dynamics simulation and Tuckerman et al.[69] using Car−Parrinello molecular dynamics simulation. The results presented above show the quality of the DC-SCC-DFTB method when compared with more accurate methods. However, the DC-SCC-DFTB method has a substantially lower computational cost when compared with these methods and allows long-time molecular dynamic simulation. It is important to highlight that this method allows the molecule polarization during the molecular dynamic simulation and this is particularly important to describe system were ions interacting with neutral molecules as in our calculations.[19]

Solvation Free Energy. In the model used in this work the solvation free energy is decomposed in two contributions. The first contribution corresponds to the interaction between solute and the nearest solvent molecules. It corresponds at the first term in eq 3. The second contribution is the long-range electrostatic interaction which is evaluated using a dielectric continuum solvation model and it corresponds to the second term in eq 3.

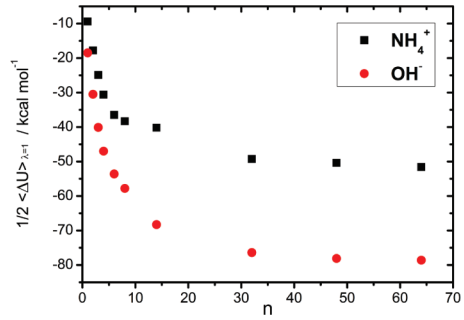

Figure 5. Inner-shell contribution for the solvation free energy of the ammonium and hydroxide ions as a function of the number of water molecules n (first term of eq 3).

In this model, the first contribution is derived from the linear response approximation and this interaction was analyzed as a function of the number of the explicit water molecules. For each structure with n water molecules the interaction energy was calculated using the PBE/6-31+G(d,p) level of theory. The results are shown in Figure 5 for both ammonium and hydroxyl ions. The standard deviation is not displayed for clarity; however, they were calculated by forming 10 sets with 50 structures each when 500 structures were selected, and 10 sets with 20 structures each when 200 structures were selected. The average of $^1/_2\langle\Delta U\rangle_{\lambda=1}$ was calculated for each group and the standard deviation was determined from these 10 average values. The standard deviation was smaller than 1.0 kcal mol^{-1} for structures with less than 64 water molecules, whereas for structures with 64 water molecules it was around 1.0 kcal mol^{-1}. We can note that this inner-shell contribution for the solvation free energy has a very high variation for some first water molecules and the slope of ($^1/_2\langle\Delta U\rangle_{\lambda=1}$) versus n becomes small around 30 water molecules. In fact, the solvation free energy has $n^{-1/3}$ dependence for large n and the convergence is very slow. Thus, the effect of outer shell is very important to reach converged values.

The outer-shell contribution was evaluated using the PCM method, through the second term of eq 3 and using different scale factors. For the first calculations we have used the default value of 1.2 for the scale factor and the results are presented in Table 2 (first column) for NH_4^+ and Table 3 for OH^-. An analysis of these tables reveals a very strange result. This contribution decreases with n, an expected result, but it becomes positive for $n \geq 32$. This is an unphysical behavior because it suggests that the ion + n solvent molecules are less solvated than the n solvent molecules. In addition, the fluctuation is large, especially for the structures with many explicit water molecules. The origin of this problem is the formation of holes inside the solute cavity, which is occupied by the dielectric continuum. When many water molecules are used, the formation of these cavities is more probable. In addition, for PCM calculations including only the solvent cluster, the hole will be present in the solute position. These holes should not be present for two reasons: first, the derivation of eq 3 considers the cavity of solute remains in the calculation of the solvent cluster; second, because the apparent surface charge method, implemented in PCM, does not allow the existence of holes inside the solute cavity. Therefore, these problems can be overcome and we have

TABLE 2: Long-Range Contribution for Solvation Free Energy of the Ammonium Ion in Aqueous Solution Calculated Using PCM with Different Scale Factor Values, with and without the Ne Atom[a,b,c]

	$\Delta G_{solv}([NH_4^+(H_2O)_n]) - \Delta G_{solv}((H_2O)_n)$									
	1.2		1.4		1.6		1.8		2.0	
n	without Ne	with Ne	without Ne	with Ne	without Ne	with Ne	without Ne	with Ne	without Ne	with Ne
1	−62.3 ± 1.7	−63.0 ± 1.6	−56.5 ± 1.4	−57.2 ± 1.3	−51.8 ± 1.1	−52.3 ± 1.1	−47.68 ± 0.89	−48.07 ± 0.84	−44.09 ± 0.74	−44.39 ± 0.69
2	−49.8 ± 2.2	−51.4 ± 2.2	−46.7 ± 1.8	−48.5 ± 2.6	−44.0 ± 1.5	−45.1 ± 1.4	−41.3 ± 1.2	−42.2 ± 1.1	−38.85 ± 0.96	−39.53 ± 0.89
3	−38.3 ± 2.9	−41.2 ± 2.8	−38.2 ± 2.3	−40.8 ± 2.2	−37.4 ± 1.9	−39.4 ± 1.8	−36.5 ± 1.5	−37.9 ± 1.4	−35.0 ± 1.2	−36.0 ± 2.5
4	−29.8 ± 3.6	−33.2 ± 3.5	−31.8 ± 2.9	−35.6 ± 2.7	−32.4 ± 2.3	−35.3 ± 2.1	−33.4 ± 1.6	−34.9 ± 1.6	−33.7 ± 1.2	−33.7 ± 1.2
6	−18.7 ± 4.7	−24.6 ± 4.0	−23.0 ± 3.6	−30.3 ± 2.9	−28.1 ± 2.5	−32.3 ± 2.1	−30.9 ± 1.6	−32.1 ± 1.5	−31.0 ± 1.1	−31.3 ± 1.1
8	−15.0 ± 4.7	−21.7 ± 6.0	−18.7 ± 5.7	−28.4 ± 4.4	−25.9 ± 3.9	−32.6 ± 2.9	−30.8 ± 2.3	−32.0 ± 2.1	−31.2 ± 1.7	−31.2 ± 1.7
14	−9.1 ± 7.8	−17.4 ± 7.2	−16.1 ± 6.6	−27.9 ± 5.7	−24.0 ± 4.4	−32.0 ± 3.3	−29.7 ± 2.3	−31.0 ± 7.5	−29.3 ± 1.7	−29.4 ± 1.7
32	9.3 ± 9.5	1.3 ± 8.5	−0.5 ± 9.6	−14.1 ± 7.7	−10.3 ± 4.6	−22.3 ± 3.7	−21.8 ± 2.6	−23.8 ± 2.2	−23.1 ± 1.5	−23.1 ± 3.2
48	12.1 ± 8.3	3.6 ± 8.8	2.7 ± 7.3	−11.6 ± 6.6	−10.2 ± 5.2	−22.3 ± 4.4	−20.6 ± 3.6	−22.7 ± 2.6	−22.1 ± 1.7	−22.3 ± 1.9
64	10.8 ± 8.8	2.3 ± 8.0	1.3 ± 7.0	−13.1 ± 5.0	−12.1 ± 4.4	−22.6 ± 2.6	−20.3 ± 2.9	−22.9 ± 1.5	−21.6 ± 1.1	−21.6 ± 1.1

[a] All values in kcal mol^{-1}. [b] A Ne atom was put in the N coordinate of the ammonium ion to calculate the $\Delta G_{solv}((H_2O)_n)$ term. [c] Each point corresponds to average on 20 structures.

TABLE 3: Long-Range Contribution for Solvation Free Energy of the Hydroxide Ion in Aqueous Solution Calculated Using PCM with Different Scale Factor Values, with and without the Ne Atom[a,b,c]

	$\Delta G_{solv}([OH(H_2O)_n]^-) - \Delta G_{solv}((H_2O)_n)$									
	1.2		1.4		1.6		1.8		2.0	
n	without Ne	with Ne	without Ne	with Ne	without Ne	with Ne	without Ne	with Ne	without Ne	with Ne
1	−72.1 ± 1.1	−71.7 ± 1.6	−63.45 ± 0.89	−63.3 ± 1.2	−56.63 ± 0.69	−56.50 ± 0.88	−51.04 ± 0.52	−50.96 ± 0.65	−46.68 ± 0.43	−46.57 ± 0.53
2	−58.2 ± 1.8	−58.5 ± 2.1	−53.0 ± 1.5	−53.5 ± 1.6	−48.5 ± 1.3	−48.9 ± 1.3	−44.49 ± 0.99	−44.78 ± 0.98	−41.37 ± 0.80	−41.54 ± 0.79
3	−47.9 ± 2.2	−49.2 ± 2.0	−45.7 ± 1.8	−46.8 ± 1.6	−43.1 ± 1.6	−43.7 ± 1.3	−40.2 ± 1.2	−40.7 ± 1.0	−37.75 ± 0.94	−37.95 ± 0.82
4	−40.4 ± 2.6	−42.9 ± 2.1	−40.9 ± 2.0	−42.6 ± 1.6	−39.4 ± 1.6	−40.6 ± 1.3	−37.4 ± 1.2	−38.0 ± 1.0	−35.18 ± 0.97	−35.52 ± 0.85
6	−30.2 ± 4.5	−34.5 ± 4.0	−34.3 ± 3.6	−36.7 ± 3.1	−34.1 ± 2.8	−35.1 ± 2.4	−34.4 ± 3.5	−34.8 ± 3.1	−31.7 ± 1.7	−31.7 ± 1.5
8	−22.9 ± 5.9	−28.4 ± 4.8	−29.2 ± 4.4	−32.7 ± 3.7	−30.9 ± 3.4	−32.6 ± 2.8	−31.3 ± 2.4	−31.6 ± 2.1	−29.8 ± 1.9	−30.0 ± 1.7
14	−3.6 ± 6.5	−10.6 ± 6.0	−15.9 ± 5.5	−21.5 ± 4.8	−21.8 ± 4.0	−24.8 ± 3.3	−25.2 ± 2.9	−25.5 ± 2.5	−25.0 ± 2.2	−24.9 ± 2.0
32	11.1 ± 6.3	3.8 ± 6.3	−4.78 ± 7.0	−11.7 ± 6.2	−15.2 ± 5.0	−18.5 ± 3.9	−19.6 ± 2.6	−20.2 ± 2.7	−20.2 ± 2.1	−19.7 ± 2.1
48	17.3 ± 7.0	9.4 ± 6.6	0.0 ± 5.4	−7.0 ± 4.6	−13.2 ± 3.6	−16.9 ± 3.1	−17.4 ± 2.7	−18.1 ± 2.1	−17.5 ± 1.9	−17.7 ± 1.7
64	17.3 ± 6.3	9.4 ± 6.2	0.2 ± 5.6	−7.0 ± 5.2	−11.7 ± 4.1	−15.8 ± 3.6	−16.8 ± 3.0	−17.4 ± 2.5	−17.1 ± 2.3	−17.0 ± 2.1

[a] All values in kcal mol^{-1}. [b] A Ne atom was put in the O coordinate of the hydroxide ion to calculate the $\Delta G_{solv}((H_2O)_n)$ term. [c] Each point corresponds to average on 20 structures.

adopted two procedures. The first problem is the solute hole, which was solved by adding one Ne atom to the hole created by the clearance of the solute. For the ammonium, Ne atom was inserted to the coordinates of the N atom, and for the hydroxyl to the coordinates of O atom. A more rigorous alternative would be to insert a sphere into the position of the solute. However, because we are using the Gamess program to perform the calculations, this approach would not be practical for this exploratory work. Nevertheless, the Ne has very small interaction with the solvent and the difference in relation to single sphere should be very small. The second problem is the holes that arise inside the water cluster. This problem can be solved increasing the scale factor. To test this effect, we have increased the scale factor from 1.2 to 2.0 and all the results are presented in Tables 2 and 3.

An analysis of different scale factors and inclusion of the Ne atom has the expected effect on the $\langle \Delta G_{solv}(NH_4(H_2O)_{48}^+) - \Delta G_{solv}((NH_4^+)(H_2O)_{48}) \rangle_{\lambda=1}$ term. Thus, this term was 12.1 ± 8.3 kcal mol^{-1} for the scale factor of 1.2 without the Ne atom. When we increase the α to 1.6, the value changes to −10.2 ± 5.2 kcal mol^{-1} without the Ne atom and to −22.3 ± 4.4 kcal mol^{-1} with the Ne atom. The scale factor of 2.0 (with and without Ne) predicts values very close to scale factor of 1.6 with Ne. Similar results have been found for the hydroxyl ion. In this way, we have calculated the long-range effects using the scale factor parameter equal to 1.6 and 2.0 with the Ne atom in the place of solute and presented the results in the Figures 6 and 7. The calculations show the convergence of the method around 32 water molecules for both systems, although even 14 water molecules are enough for the method to converge when the scale factor of 1.6 is used.

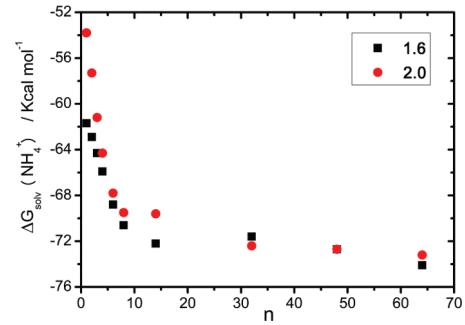

Figure 6. Solvation free energy of the ammonium ion calculated by eq 3 and using two scale factor values.

The solvation free energy for the NH_4^+ has converged to −73 kcal mol^{-1} and for the OH^- has converged to −96 kcal mol^{-1}. It is interesting to compare these values with other hybrid methods and with experimental values. In this way, Pliego and Riveros[4] have obtained the values of −79.4 and −93.1 kcal mol^{-1} for the ammonium and hydroxyl ions, respectively, using their cluster-continuum model, in reasonable agreement with our results. On the other hand, the comparison with experimental values is not trivial because it depends on the used solvation free energy scale. The Tissandier et al.[70] scale is widely adopted today, but it has become more and more evident that their scale may not be the most reliable. For example, recent computer simulations using polarizable potentials have suggested the absolute solvation free energy of the proton in water is around −250 kcal/mol, very different from the −266 kcal/mol value from Tissandier et al.[70] and close to the Marcus suggested value, based on TATB assumption.[71,72] In this work, we have adopted

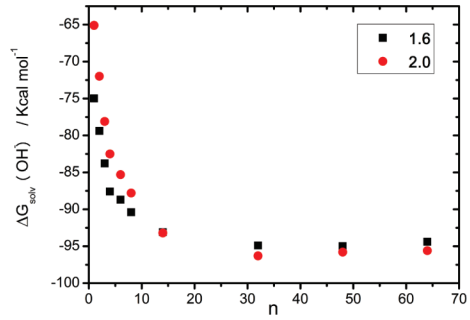

Figure 7. Solvation free energy of the hydroxide ion calculated by eq 3 and using two scale factor values.

$\Delta G_{solv}(H^+) = -251.9$ kcal mol^{-1} obtained as the average between the theoretically proposed values by Lee Warren and Patel[73] and Lamourex and Roux.[74] Thus, using this anchor value, we can estimate the experimental values as −71 and −119 kcal mol^{-1} for the solvation free energy of the ammonium and hydroxyl ions, respectively. Our calculation for the NH_4^+ cation is in excellent agreement with this experimental value. Nevertheless, for the OH^- ion, our theoretical value corresponds to only 83% of the experimental one. Why this different behavior? We can explain this result for the hydroxyl ion based on the linear response approach. In eq 3 we have neglected the $\langle U_{AS_1}\rangle_{S_1,\lambda=0}$ contribution. In fact, Grossfield[75] has shown that water molecules around a van der Waals cavity create a positive electrostatic potential inside the cavity. Thus, inclusion of this term would lead to more negative solvation free energy of the hydroxyl ion, improving the theoretical ΔG_{solv} value. On the other hand, the results for the NH_4^+ ion would be worse, leading to less negative ΔG_{solv}. Nevertheless, anyone must consider that for a full quantum mechanical treatment of solute−solvent interaction, as in this work, the solvent polarization contribution from random oriented solvent molecules could be very important. For example, in the previous paper on fluoride ion in benzene solution,[51] the $\langle U_{AS_1}\rangle_{S_1,\lambda=0}$ contribution is essentially a polarization of solvent molecules and it was estimated as amounting to 31% of the $\langle U_{AS_1}\rangle_{S_1,\lambda=1}$ term. Thus, the polarization contribution should make the solvation free energy of both the ammonium and hydroxyl ions more negative and, probably, closer to experimental value. In this point, we should emphasize that the most important aspect of this paper was to analyze the convergence of the shells theory of solvation, paying attention to the main contribution. In a future work, the method will be refined.

The shells theory of solvation has also both theoretical and practical implications, related to the long-range corrections for ion solvation. In fact, it is very usual today to perform simulations using spherical boundary conditions and to include the long-range effect through the simple Born model. However, the second term of eq 3 shows the correct expression to include the long-range effect, which is different from solvation of a charged sphere. For comparison purposes, we have made a graphics of the long-range correction through eq 3 for NH_4^+ and OH^- ions with n waters molecules and using the Born correction, through the formula

$$\Delta G_{solv} = -\frac{1}{2}\frac{1}{4\pi\varepsilon_o}\frac{q^2}{R}\left(1 - \frac{1}{\varepsilon}\right) \quad (4)$$

and

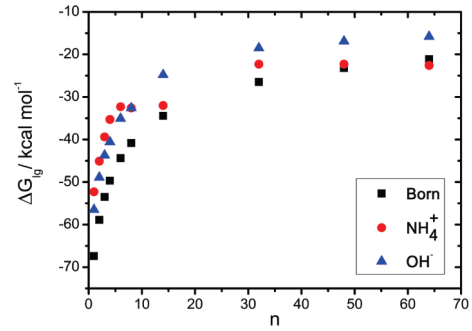

Figure 8. Outer-shell contribution for the solvation free energy of the ammonium and hydroxide ions using the shells theory of solvation (scale factor of 1.6 for PCM method) and using the Born formula for long-range correction.

$$R = 1.93(n + 1)^{1/3} \quad (5)$$

These formulas consider the volume of one water molecule as 29.9 Å^3 and R is the radius of one sphere with n water molecules plus the solute. Figure 8 shows the results. We can see the long-range correction for NH_4^+ and OH^- ions with n waters through eq 3 are different. The long-range correction is more negative for OH^- in small n and becomes less negative for n greater than 8. When the Born model is included, we can see it has a substantial deviation for small n and becomes more reliable for n from 32 to 64. However, for 64 water molecules, although the Born correction is reliable for NH_4^+ ion, the deviation for the OH^- ion is as high as 5 kcal mol^{-1}. Similar overestimation of the Born correction for the hydroxide ion in water solution was reported some time ago by Pliego and Riveros.[65] On the basis of these results, we can conclude the Born model is not reliable for including long-range corrections. Rather, the approach proposed by the shells theory of solvation presents the correct physical description of the long-range and should be used. As a final comment, the continuum method used in this paper is the most sophisticated PCM. Other approaches could be used, like the generalized Born model, which could produce fast results and be implemented in classical and quantum simulation softwares.

Conclusions

A test of a new dynamical discrete/continuum solvation model was done for hydroxide and ammonium ions in aqueous solution. A simplified linear response version of the method was analyzed and it was found this method converges when using as few as 14 water molecules and a scale factor of 1.60 for PCM calculations. For the ammonium ion, the solvation free energy was close to experimental value, whereas for the hydroxide ion, the deviation is high. It was suggested that inclusion of the omitted term of the shells theory of solvation could lead to improved values. The present work also points out that the Born model is not reliable for water solution and the present approach should be used for the long-range correction.

Acknowledgment. The authors thank the Brazilian Research Council (CNPq) and the Fundação de Amparo a Pesquisa de Minas Gerais (FAPEMIG) for the support.

References and Notes

(1) Oliveira, A. F.; Seifert, G.; Heine, T.; Duarte, H. A. *J. Braz. Chem. Soc.* **2009**, *20*, 1193.

(2) Hummer, G.; Pratt, L. R.; Garcia, A. E. *J. Phys. Chem.* **1996**, *100*, 1206.
(3) Almerindo, G. I.; Tondo, D. W.; Pliego, J. R. *J. Phys. Chem. A* **2004**, *108*, 166.
(4) Pliego, J. R., Jr.; Riveros, J. M. *J. Phys. Chem. A* **2001**, *105*, 7241.
(5) Pliego, J. R., Jr.; Riveros, J. M. *Chem. Phys. Lett.* **2002**, *355*, 543.
(6) Asthagiri, D.; Pratt, L. R.; Ashbaugh, H. S. *J. Chem. Phys.* **2003**, *119*, 2702.
(7) Bandyopadhyay, P.; Gordon, M. S.; Mennucci, B.; Tomasi, J. *J. Chem. Phys.* **2002**, *116*, 5023.
(8) Boes, E. S.; Livotto, P. R.; Stassen, H. *Chem. Phys.* **2006**, *331*, 142.
(9) Brancato, G.; Di Nola, A.; Barone, V.; Amadei, A. *J. Chem. Phys.* **2005**, *122*.
(10) Brancato, G.; Rega, N.; Barone, V. *J. Chem. Phys.* **2006**, *124*.
(11) Cossi, M.; Barone, V.; Cammi, R.; Tomasi, J. *Chem. Phys. Lett.* **1996**, *255*, 327.
(12) Cramer, C. J.; Truhlar, D. G. *Chem. Rev.* **1999**, *99*, 2161.
(13) Curutchet, C.; Bidon-Chanal, A.; Soteras, I.; Orozco, M.; Luque, F. J. *J. Phys. Chem. B* **2005**, *109*, 3565.
(14) Curutchet, C.; Cramer, C. J.; Truhlar, D. G.; Ruiz-Lopez, M. F.; Rinaldi, D.; Orozco, M.; Luque, F. J. *J. Comput. Chem.* **2003**, *24*, 284.
(15) Curutchet, C.; Orozco, M.; Luque, F. J. *J. Comput. Chem.* **2001**, *22*, 1180.
(16) Curutchet, C.; Orozco, M.; Luque, F. J.; Mennucci, B.; Tomasi, J. *J. Comput. Chem.* **2006**, *27*, 1769.
(17) da Silva, E. F.; Svendsen, H. F.; Merz, K. M. *J. Phys. Chem. A* **2009**, *113*, 6404.
(18) Gao, J. *Acc. Chem. Res.* **1996**, *29*, 298.
(19) Grossfield, A.; Ren, P. Y.; Ponder, J. W. *J. Am. Chem. Soc.* **2003**, *125*, 15671.
(20) Hofinger, S.; Zerbetto, F. *Chem.—Eur. J.* **2003**, *9*, 566.
(21) Im, W.; Berneche, S.; Roux, B. *J. Chem. Phys.* **2001**, *114*, 2924.
(22) Kelly, C. P.; Cramer, C. J.; Truhlar, D. G. *J. Chem. Theory Comput.* **2005**, *1*, 1133.
(23) Luque, F. J.; Curutchet, C.; Munoz-Muriedas, J.; Bidon-Chanal, A.; Soteras, I.; Morreale, A.; Gelpi, J. L.; Orozco, M. *Phys. Chem. Chem. Phys.* **2003**, *5*, 3827.
(24) Marenich, A. V.; Cramer, C. J.; Truhlar, D. G. *J. Phys. Chem. B* **2009**, *113*, 6378.
(25) Tomasi, J.; Mennucci, B.; Cammi, R. *Chem. Rev.* **2005**, *105*, 2999.
(26) Tse, J. S. *Annu. Rev. Phys. Chem.* **2002**, *53*, 249.
(27) Tomasi, J.; Persico, M. *Chem. Rev.* **1994**, *94*, 2027.
(28) Miertus, S.; Scrocco, E.; Tomasi, *J. Chem. Phys.* **1981**, *55*, 117.
(29) Cramer, C. J.; Truhlar, D. G. *J. Am. Chem. Soc.* **1991**, *113*, 8305.
(30) Cramer, C. J.; Truhlar, D. G. *Science* **1992**, *256*, 213.
(31) Cramer, C. J.; Truhlar, D. G. *J. Comput. Aided Mol. Des.* **1992**, *6*, 629.
(32) Cramer, C. J.; Truhlar, D. G. *J. Comput. Chem.* **1992**, *13*, 1089.
(33) Kelly, C. P.; Cramer, C. J.; Truhlar, D. G. *J. Phys. Chem. B* **2006**, *110*, 16066.
(34) Pliego, J. R., Jr.; Riveros, J. M. *J. Phys. Chem. A* **2002**, *106*, 7434.
(35) Asthagiri, D.; Pratt, L. R. *Chem. Phys. Lett.* **2003**, *371*, 613.
(36) Asthagiri, D.; Pratt, L. R.; Kress, J. D.; Gomez, M. A. *Chem. Phys. Lett.* **2003**, *380*, 530.
(37) Asthagiri, D.; Pratt, L. R.; Paulaitis, M. E.; Rempe, S. B. *J. Am. Chem. Soc.* **2004**, *126*, 1285.
(38) Rempe, S. B.; Asthagiri, D.; Pratt, L. R. *Phys. Chem. Chem. Phys.* **2004**, *6*, 1966.
(39) Westphal, E.; Pliego, J. R. *J. Chem. Phys.* **2005**, *123*.
(40) da Silva, C. O.; Barbosa, A. G. H.; da Silva, E. T.; da Silva, E. L. L.; Nascimento, M. A. C. *Theor. Chem. Acc.* **2004**, *111*, 231.
(41) de Abreu, H. A.; Guimaraes, L.; Duarte, H. A. *J. Phys. Chem. A* **2006**, *110*, 7713.
(42) de Abreu, H. A.; Guimaraes, L.; Duarte, H. A. *Int. J. Quantum Chem.* **2008**, *108*, 2467.
(43) Guimaraes, L.; de Abreu, H. A.; Duarte, H. A. *Chem. Phys.* **2007**, *333*, 10.
(44) Kelly, C. P.; Cramer, C. J.; Truhlar, D. G. *J. Phys. Chem. A* **2006**, *110*, 2493.
(45) Li, J.; Fisher, C. L.; Chen, J. L.; Bashford, D.; Noodleman, L. *Inorg. Chem.* **1996**, *35*, 4694.
(46) Zhao, Y. L.; Meot-Ner, M.; Gonzalez, C. *J. Phys. Chem. A* **2009**, *113*, 2967.
(47) Almlof, M.; Carlsson, J.; Aqvist, J. *J. Chem. Theory Comput.* **2007**, *3*, 2162.
(48) Aqvist, J.; Hansson, T. *J. Phys. Chem.* **1996**, *100*, 9512.
(49) Ben-Amotz, D.; Underwood, R. *Acc. Chem. Res.* **2008**, *41*, 957.
(50) Carlson, H. A.; Jorgensen, W. L. *J. Phys. Chem.* **1995**, *99*, 10667.
(51) Pliego Jr., J. R. *Theor. Chem. Acc.*, in press.
(52) Frisch, M. J.; Trucks, G. W.; Schlegel, H. B.; Scuseria, G. E.; Robb, M. A.; Cheeseman, J. R.; Montgomery, J., J. A.; Vreven, T.; Kudin, K. N.; Burant, J. C.; Millam, J. M.; Iyengar, S. S. T. J.; Barone, V.; Mennucci, B.; Cossi, M.; Scalmani, G.; Rega, N.; Petersson, G. A.; Nakatsuji, H.; Hada, M.; Ehara, M.; Toyota, K.; Fukuda, R.; Hasegawa, J.; Ishida, M.; Nakajima, T.; Honda, Y.; Kitao, O.; Nakai, H.; Klene, M.; Li, X.; Knox, J. E.; Hratchian, H. P.; Cross, J. B.; Bakken, V.; Adamo, C.; Jaramillo, J.; Gomperts, R.; Stratmann, R. E.; Yazyev, O.; Austin, A. J.; Cammi, R.; Pomelli, C.; Ochterski, J. W.; Ayala, P. Y.; Morokuma, K.; Voth, G. A.; Salvador, P.; Dannenberg, J. J.; Zakrzewski, V. G.; Dapprich, S.; Daniels, A. D.; Strain, M. C.; Farkas, O.; Malick, D. K.; Rabuck, A. D.; Raghavachari, K.; Foresman, J. B.; Ortiz, J. V.; Cui, Q.; Baboul, A. G.; Clifford, S.; Cioslowski, J.; Stefanov, B. B.; Liu, G.; Liashenko, A.; Piskorz, P.; Komaromi, I.; Martin, R. L.; Fox, D. J.; Keith, T.; Al-Laham, M. A.; Peng, C. Y.; Nanayakkara, A.; Challacombe, M.; Gill, P. M. W.; Johnson, B.; Chen, W.; Wong, M. W.; Gonzalez, C.; and Pople, J. A. *Gaussian 03; Revision D.01.*; Gaussian, Inc.: Wallingford, CT, 2004.
(53) Perdew, J. P.; Burke, K.; Ernzerhof, M. *Phys. Rev. Lett.* **1997**, *78*, 1396.
(54) Becke, A. D. *Phys. Rev. A* **1988**, *38*, 3098.
(55) Lee, C. T.; Yang, W. T.; Parr, R. G. *Phys. Rev. B* **1988**, *37*, 785.
(56) Elstner, M. *Theor. Chem. Acc.* **2006**, *116*, 316.
(57) Zhechkov, L.; Heine, T.; Patchkovskii, S.; Seifert, G.; Duarte, H. A. *J. Chem. Theory Comput.* **2005**, *1*, 841.
(58) Aradi, B.; Hourahine, B.; Frauenheim, T. *J. Phys. Chem. A* **2007**, *111*, 5678.
(59) Koster, A. M.; Flores, R.; Gludtner, G.; Goursot, A.; Heine, T.; Patchkovskii, S.; Reveles, J. U.; Vela, A.; Salahub, D. R. deMon. NRC: Ottawa, Canadá, 2004.
(60) Berendsen, H. J. C.; Postma, J. P. M.; Vangunsteren, W. F.; Dinola, A.; Haak, J. R. *J. Chem. Phys.* **1984**, *81*, 3684.
(61) Cances, E.; Mennucci, B.; Tomasi, J. *J. Chem. Phys.* **1997**, *107*, 3032.
(62) Miertus, S.; Tomasi, *J. Chem. Phys.* **1982**, *65*, 239.
(63) Schmidt, M. W.; Baldridge, K. K.; Boatz, J. A.; Elbert, S. T.; Gordon, M. S.; Jensen, J. H.; Koseki, S.; Matsunaga, N.; Nguyen, K. A.; Su, S. J.; Windus, T. L.; Dupuis, M.; Montgomery, J. A. *J. Comput. Chem.* **1993**, *14*, 1347.
(64) Intharathep, P.; Tongraar, A.; Sagarik, K. *J. Comput. Chem.* **2005**, *26*, 1329.
(65) Pliego, J. R.; Riveros, J. M. *J. Phys. Chem. B* **2000**, *104*, 5155.
(66) Pliego, J. R.; Riveros, J. M. *J. Chem. Phys.* **2000**, *112*, 4045.
(67) Bruge, F.; Bernasconi, M.; Parrinello, M. *J. Am. Chem. Soc.* **1999**, *121*, 10883.
(68) Asthagiri, D.; Pratt, L. R.; Kress, J. D.; Gomez, M. A. *Proc. Natl. Acad. Sci. U.S.A.* **2004**, *101*, 7229.
(69) Tuckerman, M. E.; Marx, D.; Parrinello, M. *Nature* **2002**, *417*, 925.
(70) Tissandier, M. D.; Cowen, K. A.; Feng, W. Y.; Gundlach, E.; Cohen, M. H.; Earhart, A. D.; Coe, J. V.; Tuttle, T. R. *J. Phys. Chem. A* **1998**, *102*, 7787.
(71) Marcus, Y. *J. Chem. Soc., Faraday Trans.* **1987**, *83*, 2985.
(72) Marcus, Y. *J. Chem. Soc., Faraday Trans.* **1991**, *87*, 2995.
(73) Warren, G. L.; Patel, S. *J. Chem. Phys.* **2007**, *127*.
(74) Lamoureux, G.; Roux, B. *J. Phys. Chem. B* **2006**, *110*, 3308.
(75) Grossfield, A. *J. Chem. Phys.* **2005**, *122*.

JP110202E